

**PSFC/JA04-27**

**Internal Transport Barrier Production and Control  
in Alcator C-Mod**

C.L. Fiore, P.T. Bonoli, D.R. Ernst, M.J. Greenwald, E.S. Marmor,  
M.H. Redi,<sup>a</sup> J.E. Rice, S.J. Wukitch, K. Zhurovich

July 14, 2004

Plasma Science and Fusion Center  
Massachusetts Institute of Technology  
Cambridge, MA 02139 USA

<sup>a</sup> present address: Princeton Plasma Physics Laboratory, Princeton, NJ

This work was supported by the U.S. Department of Energy, Cooperative Grant No. DE-FC02-99ER54512. Reproduction, translation, publication, use and disposal, in whole or in part, by or for the United States government is permitted.

Submitted for publication to *Plasma Physics and Controlled Fusion*.

## Internal Transport Barrier Production and Control in Alcator C-Mod

C.L. Fiore<sup>1</sup>, P. T. Bonoli<sup>1</sup>, D. R. Ernst<sup>1</sup>, M. J. Greenwald<sup>1</sup>, E. S. Marmor<sup>1</sup>, M. H. Redi<sup>2</sup>,  
J. E. Rice<sup>1</sup>, S. J. Wukitch<sup>1</sup>, K. Zhurovich<sup>1</sup>

<sup>1</sup>Plasma Science and Fusion Center, Massachusetts Institute of Technology, Cambridge,  
MA 02139;

<sup>2</sup>Princeton Plasma Physics Laboratory, Princeton, NJ

### **Abstract**

Internal transport barriers, marked by a steep density profile, even stronger peaking in the pressure profile and reduction of core transport are obtained in Alcator C-Mod. They are induced by the use of off-axis D(H) ICRF power deposition. They also arise spontaneously in Ohmic H-mode plasmas when the H-mode lasts for several energy confinement times. Recent studies have explored the limits for forming, maintaining, and controlling these plasmas. C-Mod provides a unique platform for studying such discharges: the high density (up to  $8 \times 10^{20}/\text{m}^3$ ) causes the ions and electrons to be tightly coupled by collisions with  $T_i/T_e=1$ , and the plasma has no internal particle or momentum sources. The ITBs formed in both Ohmic and ICRF heated plasmas are quite similar regardless of the trigger method. Control of impurity influx and heating of the core plasma in the presence of the ITB have been achieved with the addition of central ICRF power, in both Ohmic H-mode and ICRF induced ITBs. Control of the radial location of the transport barrier is achieved through manipulation of the toroidal magnetic field and plasma current. A narrow region of decreased electron thermal transport, as determined by sawtooth heat pulse analysis, is found in these plasmas as well. Transport analysis

indicates that reduction of the particle diffusivity in the barrier region allows the neoclassical pinch to drive the density and impurity accumulation in the plasma center. Examination of the gyrokinetic stability indicates that the density and temperature profiles of the plasma core are inherently stable to long- wavelength drift mode driven turbulence at the onset time of the ITB, but that the increasing density gradients cause the trapped electron mode (TEM) to play a role in providing a control mechanism to ultimately limit the steepness of the density gradient in the ITB region.

## **1. Introduction**

Regions of reduced energy, particle, and/or momentum transport have been observed in a large number of toroidal plasma experiments throughout the world, under a variety of different conditions. The edge transport barrier which gives rise to the enhanced confinement regime known as H-mode[1] is ubiquitous in toroidal plasmas and forms the benchmark for optimized plasma performance. Transport barriers are widely reported to occur in the plasma interior as well, usually under very specific operational conditions. A comprehensive review of the internal transport barrier experiments and analysis can be found in recent papers by Wolf[2] and Connor[3].

An early observation of a particle transport barrier accompanied by improved energy confinement was found with pellet injection on Alcator C[4] and has since been reported using lithium pellets in combination with ICRF heating on Alcator C-Mod [5], as was first seen in JET[6]. Most commonly, transport barriers in the plasma interior are found in neutral beam heated plasmas [2], where the beam provides a source of particles and momentum to the plasma. The resulting rotation of the plasma is thought to generate sufficient electric field shear to stabilize microinstabilities such as the ion temperature

gradient driven instability (ITG) by increasing the E X B shearing rate above the maximum linear growth rate for the instability. Other techniques utilizing radio frequency waves to alter the internal magnetic configuration of the plasma to obtain magnetic shear stabilization of such instabilities through techniques such as lower hybrid current drive[7,8], ion Bernstein wave injection[2] and electron cyclotron heating[2] have also been demonstrated.

Internal transport barriers produced in Alcator C-Mod are unusual in that they arise in H-mode plasmas that have enhanced  $D_{\alpha}$  emission from the plasma edge (known as EDA H-modes[9]). These have no imposed momentum or particle sources and do not rely on reversed or extremely low magnetic shear[10,11,12,13]. They can be induced with the use of off-axis ICRF heating, but they have also been observed to arise in purely Ohmic H-mode discharges. They are most noticeable in the particle transport channel, in that a strong increase in central density is seen as they develop. At the same time, there is no decrease in the core ion and electron temperatures, so that there is a net strong peaking of the plasma pressure, providing evidence for a thermal barrier as well[12,13]. Despite the absence of externally applied torque, the central plasma rotation measured from the Doppler shift of argon impurity lines typically slows down from its nominally co-going value typical of Alcator C-Mod H-mode plasmas and reverses direction, coincident with the ITB development and growth[10,13,14].

Success in controlling the rise of the central density and the accompanying central impurity accumulation with tailored application of central ICRF heating after the development of the ITB has been recently reported[13,15], although limits on the maximum amount of power which could be added were found. Recent experiments have

explored the effects of varying the input power profiles to the plasma, resulting in the extension of the operational parameters and significant improvement of the performance of Alcator C-Mod ITB plasmas. Control of the ITB location by variation of the plasma current and magnetic field has been extended. These new results and further discussion of the underlying physics will be presented.

## **2. The experimental set up and diagnostics**

The Alcator C-Mod tokamak is a high field ( $B_T$  up to 8.1 T),  $R/a=0.67/0.22$  m tokamak [16]. Plasma currents up to 2 MA have recently been achieved. Typical operation is for central electron density of between  $1 \times 10^{20}$  up to  $8.0 \times 10^{20} \text{ m}^{-3}$  or higher after ITB development with gas fueling alone. Normal operation uses a lower single null, although ITB plasmas have been obtained in the double null configuration. The walls consist of molybdenum tiles that are coated with a thin layer of boron through discharge cleaning in dilute diborane gas every one to two weeks.

Currently the only source of auxiliary heating in the plasma comes from up to 6 MW ICRF power. This is supplied to the plasma through 3 antennas: 2 double strap and one 4 strap [17]. The 2 double strap antennas have fixed frequency at 80 MHz while the 4 strap system can be driven with 50, 70, or 78 MHz. with a total source power of up to 6 MW for the 3 combined. For these experiments, the ICRF system is configured for heating phasing and makes use of a hydrogen minority (~4%) in a deuterium majority. A combination of on and off-axis ICRF resonances are used for the experiments presented here, using the frequencies listed above at different magnetic fields to vary the resonance positions.

H-mode operation is routinely obtained in Alcator C-Mod and spans the full operational range of the device, with line averaged density up to  $4.8 \times 10^{20} \text{ m}^{-3}$ [18] (no ITB). They are routinely seen in both purely Ohmic heated discharges as well as during ICRF powered plasmas. Most operation occurs without the appearance of edge localized modes (ELMs), and is either ELM-free or shows enhanced  $D_\alpha$  emission (EDA)[9] during the H-mode. The plasmas, presented in this paper, were all EDA H-modes, which tend to give more reproducible and steadier performance as well as lasting longer than typical ELM-free H-modes.

Alcator C-Mod is equipped with an extensive set of standard core diagnostics. The results reported here use data from the following systems: Electron temperature profiles are obtained from two grating polychromator electron cyclotron emission (ECE)diagnostics, one with 9 and the other with 18 spatial channels[19] as well as with a high resolution heterodyne ECE radiometer which provides 32 channels at 7 mm spacing[20]. Eleven spatial points of electron density and temperature are obtained using Thomson scattering in the core of the plasmas ( a second system provides edge  $T_e$  and  $n_e$  profiles.) Density profiles with high spatial and temporal resolution can also be derived from a CCD based one-dimensional imaging system measuring visible bremsstrahlung emission from the plasma with 208 spatial channels[21]. The square root of this emission, after correction for a weak dependence on electron temperature, is equal to  $n_e \sqrt{Z_{\text{eff}}}$  . Assuming that the radial profile of  $Z_{\text{eff}}$  is flat across the profile, as is typical for Alcator C-Mod plasmas, the density profile can be obtained with a high level spatial resolution. An 11 point spatial  $Z_{\text{eff}}$  profile during the ITB development is obtained by comparison of the square root of the visible bremsstrahlung emission to the density

profiles obtained from Thomson scattering. Measurements of central toroidal plasma rotation are obtained from x-ray spectra recorded by a spatially fixed, tangentially viewing, von Hamos type crystal x-ray spectrometer[22] and confirmed independently from frequency analysis of sawtooth pre- and post-cursors[23].

### **3. Characteristics of Alcator C-Mod ITBs**

The most pronounced feature of the ITB profile on Alcator C-Mod is an extremely peaked electron pressure profile, which arises gradually over 0.1 to 0.2 s after the H-mode transition (typical energy confinement time is 0.04 s) in plasmas where the input power is not centrally peaked. An example is shown in Fig.1 of an ITB that was formed from such a plasma using 3 MW ICRF power injected off-axis on the low-field side of the plasma. The ICRF is applied at  $t=0.6$  s and the plasma goes into H-mode almost immediately. The central pressure begins peaking by  $\sim 0.8$  s and continues rising until an RF fault occurs at 1.3 s, corresponding to the end of the H-mode. The electron pressure profiles measured with Thomson scattering are shown before and during the ITB development in Fig 2.

Profiles of the visible bremsstrahlung emission during the rise of the ITB are displayed in Fig.3 for the same discharge pictured in Figs. 1 and 2. The high spatial resolution of this diagnostic allows the break in the slope of the profile, which occurs at the barrier foot, to be seen clearly. The relatively flat density profile, characteristic of Alcator C-Mod H-mode plasmas, is seen to begin peaking in the plasma center at  $t= 1$  s, which is 0.4 s or 10 energy confinement times after the onset of the H-mode. These profiles continue to peak for another 0.3 s, when the core  $Z_{\text{eff}}$  rises sharply and the plasma undergoes a back-transition out of H-mode; likely caused by a radiative collapse of the

central temperature. The time history (Fig 4.a.) and radial profiles (Fig 4.b) of the  $Z_{\text{eff}}$ , derived from the square of the ratio of the square root of the visible bremsstrahlung data to the local electron density measurement obtained from Thomson scattering, are shown for this discharge. It is apparent that in this case the  $Z_{\text{eff}}$  profiles are relatively flat, between 1 and 2 for most of the discharge and that significant impurity accumulation in the center occurs only at the very end of the ITB lifetime, just before it collapses.

Analysis of sawtooth data on the soft x-ray emission has shown that there is a significant delay in the propagation of the heat pulse which occurs at the sawtooth crash across the barrier region[12]. This is best modeled by a narrow region (<0.02 m) of reduced electron heat transport at or near the foot of the ITB as determined from the electron density profile. This is interpreted as a decrease in the incremental electron heat conductivity and it has been found to be of the order of  $0.1 \text{ m}^2/\text{s}$  at the barrier.

An examination of the particle and thermal transport characteristics of the ITB discharges [15] indicates that the effective heat coefficient,  $\chi_{\text{eff}}$ , decreases as the ITB develops and becomes equivalent to the neoclassical (Chang-Hinton [24]) value of ion thermal conductivity  $\chi_i$  in the core region of the plasma. The H-mode value of 1.1 to 1.4  $\text{m}^2/\text{s}$  drops to between 0.1 and 0.2  $\text{m}^2/\text{s}$  in the core region of the plasma at radii  $< r/a=0.4$ . This analysis is performed through the use of the TRANSP code[25] and uses the experimentally determined electron density and temperature profiles, employing a variable multiplier on the Chang-Hinton value of  $\chi_i$  to obtain the ion temperature profile consistent with the measured neutron rate. The ion temperature obtained in this manner is very close to the electron temperature measured for these plasmas and is consistent with the central ion temperature obtained from inverting the global neutron emission with



the electron density profile assuming an ion temperature profile similar to that of the electron temperature. Separation of the ion and electron transport channels is nearly impossible due to large uncertainty in the exchange term, so that

$$\chi_{eff} \equiv \frac{n_e \chi_e \nabla T_e + n_i \chi_i \nabla T_i}{n_e \nabla T_e + n_i \nabla T_i}$$

is used for the measure of the plasma heat transport.

Further, exploration of the particle transport indicates that the particle diffusivity decreases as an ITB develops to a level similar to  $\chi_{eff}$  in the core region[26]. This decrease in the outward particle diffusion allows the inward neoclassical pinch term to dominate the transport and is sufficient to account for the experimentally observed central density increase. The neoclassical pinch velocity is relatively large in Alcator C-Mod because its small size and low electron temperature yields a larger toroidal electric field.

## **4. Extension of Operation and Control**

### **4.1 ITB formation and central power deposition**

It has been established that the density rise and impurity accumulation that occurs with the development of an ITB in Alcator C-Mod can be halted with the addition of central ICRF power[12,13]. This has been demonstrated for ITBs created with off-axis ICRF heating as well as for those arising spontaneously from Ohmic H-mode EDA conditions[15]. It was also found that there was an apparent, relatively low power limit (~0.8 MW) to how much additional ICRF power could be added without degrading or destroying the ITB profile. Recent ITB experiments, which used a higher level of off-axis ICRF power, have allowed a higher level of central ICRF power to be added without terminating the ITB. At this point, there is no observed limit to adding central ICRF power to an established ITB plasma. Increasing the central power resulted in strong central heating of the plasma and record plasma pressure for Alcator C-Mod. The plasma

performance parameters are shown in Fig. 5, and the electron pressure profiles are demonstrated in Fig. 6.

A sharp threshold for ITB formation has been observed in the off-axis ICRF heated cases with applied toroidal magnetic field and the ICRF resonance located on either the low or high field side of the plasma[10,13]. To further test this sensitivity and the extent of any hysteresis, an experiment was done to test for the sharpness of this boundary. First, an H-mode is established using off-axis ICRF power at a toroidal magnetic field value which locates the ICRF resonance too close to the center for ITB development. The magnetic field is then ramped down, which moves the resonance farther towards the high field side of the plasma, effectively to larger  $r/a$  position, until an ITB is produced. The converse is also done, in which an ITB is established in an off-axis ICRF heated plasma. The toroidal magnetic field is then ramped up until the ITB profile is lost. Since the location of the ICRF power deposition is changed with the magnetic field ramp, it seems reasonable to suggest that the most important factor in this test is the relative amount of power located inside/outside of the ITB radius. The results of a calculation of the total of the Ohmic and ICRF power distribution in these plasmas as calculated by using TRANSP, in which the TORIC code[27] calculation of ICRF deposition is coupled with a Fokker-Planck solver to obtain a solution, are shown in Fig. 7. It is seen that an ITB forms in these experiments when the power inside the ITB radius is roughly less than 40% of the total input and that the ITB terminates when the power inside the ITB radius exceeds 60% of the total. The high performance discharge featured in Figs. 5 and 6 is consistent with this limit, in that the net power inside the ITB radius was  $\approx 50\%$  of the total.

## 4.2 Plasma Rotation

Typical Alcator C-Mod H-mode plasmas demonstrate strong co-going central plasma rotation with intensity dependent upon the plasma stored energy and the current [28]. It has been widely reported that this co-going rotation slows and reverses to the counter direction as a typical ITB develops in these plasmas[10,12,13]. The role of the rotation in the formation of the ITB is probably not important for two reasons: initially the ITB profile begins to build up when the plasma is in H-mode. The apparent velocity profiles at that time are typically flat from  $0 < r/a < 0.6$ [29], which is slightly outside of the ITB foot position  $r/a \approx 0.45$ , although velocity shear in the ITB region has been found in cases during high field side off-axis ICRF heating after the ITB is fully developed[30].

Recent measurements of the central plasma rotation at higher magnetic field with the ICRF resonance place on the low field side of the plasma do not appear to reproduce this earlier result. The rotation for high and low field side resonance conditions from recent experiments are compared in Fig.8. In the high field side resonance case, the central rotation level decreases from the time the H-mode starts and becomes strongly counter as the ITB develops. For the low field side resonance, the rotation is strongly co-going but then decreases somewhat as the ITB develops. It does not decrease all the way to zero. However, the absolute value of the change is comparable in the two cases. It should be noted that the plasma stored energy is higher than is usually seen in ITBs in the second case because the off-axis ICRF power was higher than has been used in previous Alcator C-Mod ITB experiments. As was noted earlier, strong co-going rotation in Alcator C-mod is correlated with increasing the plasma pressure and stored energy.

## 4.3 ITB foot location dependence on magnetic field

The location of the ITB foot in Alcator C-Mod has been shown to narrow with increasing toroidal magnetic field[14]. Results found by scanning the plasma current with a fixed magnetic field suggested that the foot position moved outward with increasing current [15]. The current dependence has now been tested at high magnetic field as well, and the result is shown in Fig 9.a. A clear trend with both increasing plasma current and decreasing magnetic field is demonstrated. Fitting the data with a power law to these quantities results in  $r/a$  at the foot position  $\sim I_p^{0.94} B_t^{-1.13}$ . Since the  $q$  profile of the plasma depends upon the ratio of these quantities, the data is also plotted a function of  $q_{95}$  in Fig. 9.b., showing a linear dependence of the ITB foot position with decreasing  $q_{95}$ . Comparison with the calculated  $q$  profile determined by EFIT shows that the typical ITB location lies between a  $q$  value of 1.1 and 1.34. (Note that these discharges are sawtoothing, so that the sawtooth inversion radius is well determined to be inside of the ITB foot location.)

## 5.0 Modeling and analysis

A typical off-axis ICRF heated H-mode plasma in Alcator C-Mod has been modeled using linear gyro-kinetic stability analysis with the computer code GS2[31] at the time when an ITB is beginning to form. It was concluded that there are no long-wavelength drift modes present in the core at this point in time[32] and that the temperature profile is just below marginal stability[26]. The ion temperature gradient mode has a finite growth rate at the barrier location at the onset time and is strongly growing outside of the barrier where the density gradient is near zero[32].

The peaking of the plasma density is thought to result when the core turbulent transport declines and the particle diffusivity decreases to a value near that of the

effective heat diffusivity  $\chi_{\text{eff}}$ [26]. The neoclassical (or Ware) pinch velocity is sufficiently strong in Alcator C-Mod to account for the central peaking of the density without requiring any anomalous pinch. The increasing density profile gradient is further stabilizing to toroidal  $\eta_i$  or ion temperature gradient modes but at the same time is destabilizing to trapped electron modes (TEM) in the barrier region, as has been demonstrated with further gyro-kinetic stability analysis[26]. Eventually the TEM driven turbulent transport in the barrier balances the neoclassical pinch and the density gradient no longer increases. The addition of central ICRF power in the core contributes to the magnitude of the TEM driven turbulent transport at the center, which then completely balance the neoclassical pinch and halts any further central density rise[26], thus providing a control mechanism.

## **6. Discussion and Future Work**

Internal transport barriers form spontaneously in the pressure profiles in Alcator C-Mod EDA H-mode plasmas if the input power profile is broadly distributed across the plasma rather than centrally peaked. These are formed in the absence additional particle or momentum sources injected into the plasma. While these have only been seen in EDA H-modes, it is thought that the relevant parameter is the steadiness of the H-mode (ELM free H-modes tend to have frequent back-transitions in Alcator C-Mod) and that it has to last long enough for the neoclassical pinch velocity to peak the central density. Once the central density and impurities begin to peak, they will generally continue to rise until the plasma suffers a radiative collapse.

It has been demonstrated, however, that the addition of central ICRF power into an established ITB plasma will control the further rise of the central particle and impurity

accumulation, likely through amplifying the trapped electron mode (TEM) driven turbulent transport. A bonus of this process is the increase in the central temperature, pressure and fusion rate in the core. Doubling of the central temperature and pressure and 10-fold increase in the fusion rate have been achieved.

The ITB foot location has been determined to depend on increasing plasma current and decreasing toroidal magnetic field, making it likely that the functional dependence is on the safety factor or magnetic shear.

The Alcator C-Mod program will begin operation of lower-hybrid wave current drive (LHCD) experiments in fall 2004. This will allow further exploration of the effects of tailoring of the q-profile on the ITB foot position. It will also provide information on the role of the neoclassical pinch in establishment of these ITBs, since this pinch is driven by the parallel electric field which can be minimized or eliminated in LHCD experiments. Recent upgrades in fluctuation diagnostics are expected to soon provide information on the role of turbulent transport in these plasmas as well.

### **Acknowledgements**

This work is supported by D.o. E. Coop. Agreement DE-FC02-99ER54512. The authors would like to thank Amanda Hubbard (MIT), Alan Lynn and Perry Phillips (FRC, UT Austin) for high resolution electron temperature data, Dimitri Mossessian and Jerry Hughes for Thomson scattering density and pressure profiles. They would also like to thank Steve Wolfe, Joe Snipes, Bob Granetz, Ron Parker, Bill Rowan, and Jim Irby for their expert operation of the tokamak for many of the experiments presented here, Yijun Lin for operation of the ICRF system and also the Alcator C-Mod Operations Group for their support of this work.

## References

- [1]ASDEX Team, 1989 *Nucl. Fusion* **29** 1959
- [2]Wolf R C 2003 *Plasma Physics and Controlled Fusion* **45** R1
- [3]Connor J W *et al* 2004 *Nucl. Fusion* **44** R1
- [4]Greenwald M J *et al.* 1984 *Phys. Rev. Lett.* **53** 352
- [5]Garnier D T *et al* 1996 *Proc. of the 16th International Conference on Fusion Energy* (Montreal,1996) (International Atomic Energy Agency, Vienna,1997), Vol. I,90.
- [6]Hugon, M *et al* 1992 *Nucl. Fusion* **35** 33
- [7]Pericoli Ridolfini V *et al* 2003 *Nucl. Fusion* **6** 469
- [8]Fujisawa A *et al* 1999 *Phys. Rev. Lett.* **82** 2669
- [9]Greenwald M J *et al* 1999 *Phys. Plasmas* **6** 1943
- [10]Rice J E *et al* 2001 *Nucl. Fusion* **41** 277
- [11]Fiore C L *et al* 2001 *Phys Plasmas* **8** 2023
- [12]Wukitch S J *et al* 2002 *Phys. Plasmas* **9** 2149
- [13]Rice J E *et al* 2002 *Nucl. Fusion* **42** 510
- [14]Rice JE *et al* 2003 *Nucl. Fusion* **43** 781
- [15]Fiore C L *et al* 2004 *Phys. Plasmas* **10** 2480
- [16]Hutchinson I H *et al* 1999 *Plasma Phys. Control. Fusion* **41** A609
- [17]Wukitch S J *et al* 2002 *Proc. Of the 19<sup>th</sup> IAEA Fusion Energy Conference* (IAEA, Vienna,2002) FT/P1
- [18]Greenwald M *et al* 1997 *Nucl. Fusion* **37** 793
- [19]Hubbard A E *et al* 1998 *Phys. Plasmas* **5** 1745
- [20]Chatterjee R *et al* 2001 *Fus. Eng. Des.* **53** 113

- [21]Marmor E S *et al* 2001 *Rev. Sci. Instrum.***72** 940
- [22]Rice J E *et al* 1999 *Nucl. Fusion* **39** 1175
- [23]Hutchinson I *et al* 2000 *Phys. Rev. Lett.* **84** 3330
- [24]Chang C S and Hinton F L 1982 *Phys. Fluids* **25** 1493
- [25]Hawryluk, R 1979 in *Physics of Plasma Close to Thermonuclear Conditions* (Varenna,1979), Commission of the European Communities, Brussels, Vol. I p 61
- [26]Ernst D R *et al* 2004 *Phys. Plasmas* **10** 2637
- [27]Brambilla M 1999 *Plasma Phys. Controlled Fus.* **41** 1
- [28]Rice J E *et al* 1998 *Nucl. Fusion* **38** 75
- [29]Lee W D *et al* 2003 *Phys Rev. Lett.* **91** 205003
- [30]Rice J E *et al* 2004 *Nucl. Fusion* **44** 379
- [31]Kotschenreuther M *et al* 1995 *Comput. Phys. Commun.* **88** 129
- [32]Redi M H *et al.*, Proceedings EPS (2004) London, England Paper 2-163

## Figures

Fig 1. The time history of the electron pressure is shown as the ITB develops. The ICRF power is applied at  $t=0.6$  s, and the plasma goes into H-mode almost immediately. The central pressure begins peaking by  $\sim 0.8$  s, and continues rising until an ICRF fault occurs at 1.3 s, ending the H-mode.

Fig. 2. The electron pressure profiles measured with Thomson scattering are shown during the ITB development for the plasma in Fig. 1.



Fig. 3. The profiles of the square root of the visible bremsstrahlung emission is shown for the same discharge as in Fig. 1 and Fig 2.

Fig. 4. The  $Z_{\text{eff}}$  derived from taking the square of the ratio of the square root of the visible bremsstrahlung emission to the electron density from Thomson scattering is shown as a function of (a) time and (b) major radius.

Fig 5. Several plasma parameters are shown as a function of time for an ITB which was created with 2.3 MW off-axis ICRF power which was then heated with an additional 1.7 MW of power deposited at the plasma center. The electron pressure doubles, stored energy increases, neutron rate increases 10-fold, central electron and ion temperatures double.

Fig. 6 Electron pressure profiles for the discharge of Fig. 5 are shown as the ITB develops.

Fig. 7 The toroidal magnetic field is ramped either up or down (a) moving the ICRF resonance towards or away from the center of the plasma. The percentage of power inside the ITB radius (b) changes with the resonance position and the point where an ITB is either formed or lost is indicated.

Fig. 8. Central toroidal rotation measured from Argon impurity ions are shown as a function of time for two off-axis ICRF generated ITB plasmas, one at 4.5 T with high field side deposition of 80 MHz, and the other at 6.3 T with low field side deposition.

Fig. 9. The ITB foot position increases with plasma current for scans made at two different magnetic fields (a). The foot position decreases with increasing  $q_{95}$  (b).

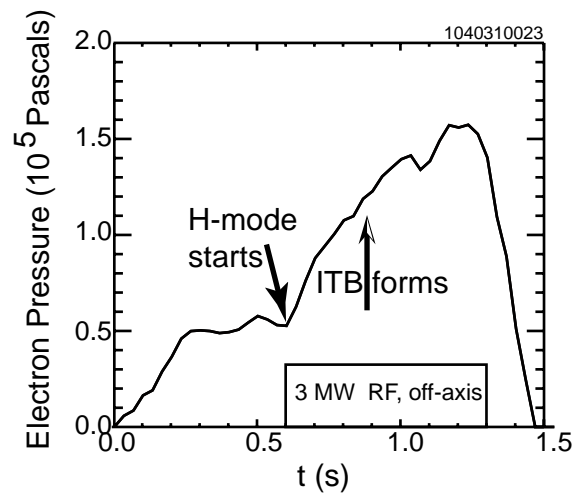


Fig 1.

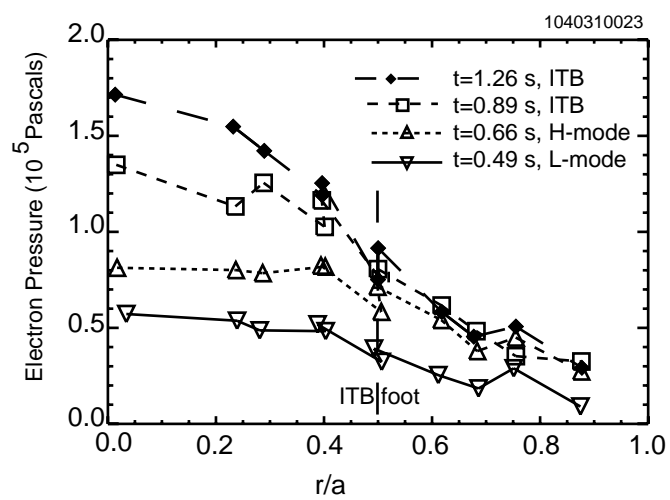
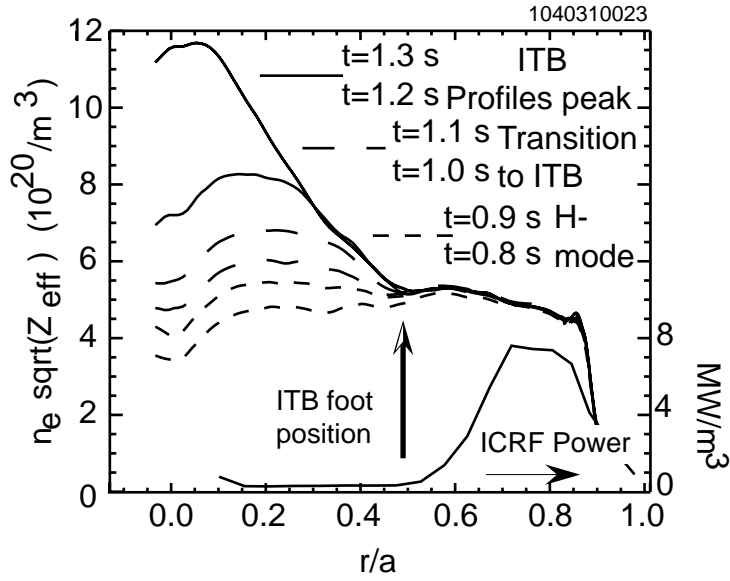
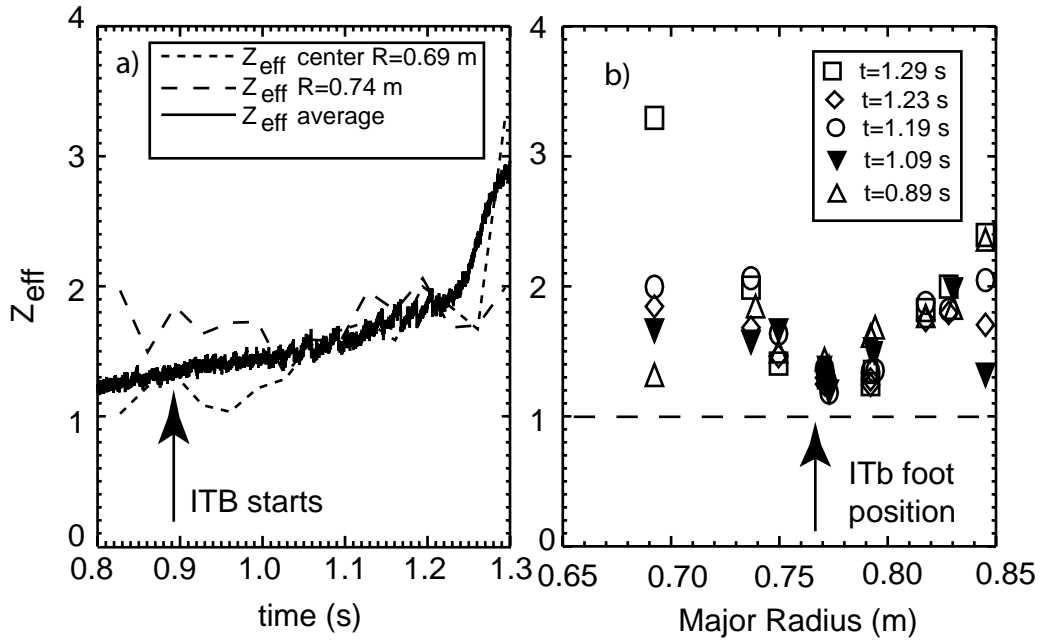


Fig. 2.



**Fig. 3**



**Fig. 4.**

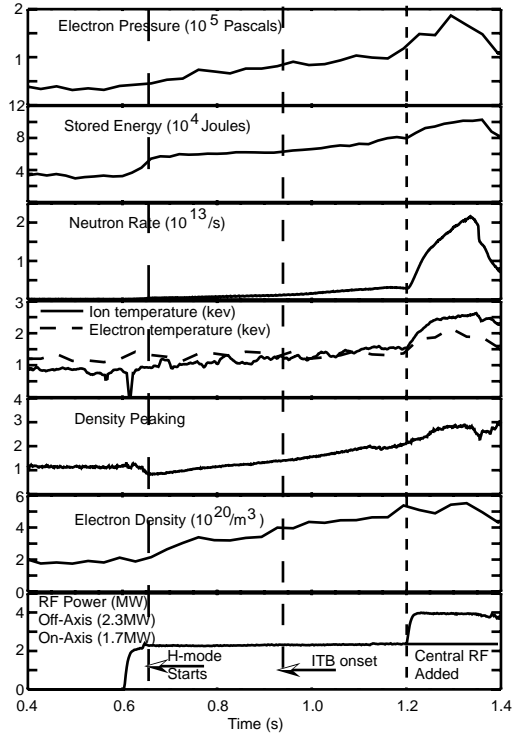


**Fig 5.**

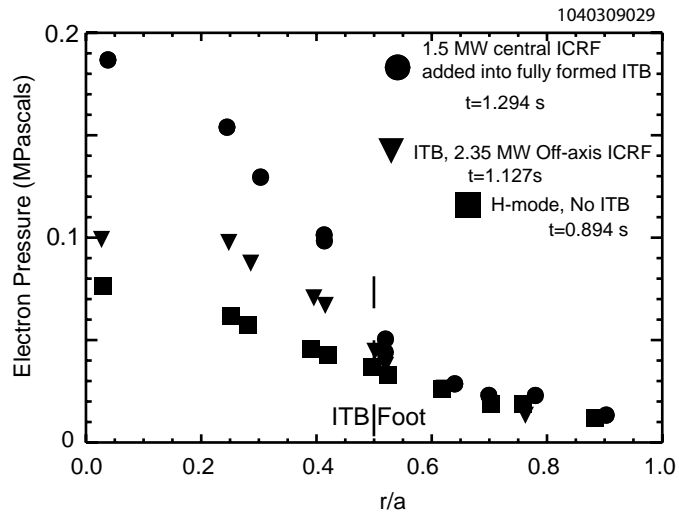


**Fig 6.**

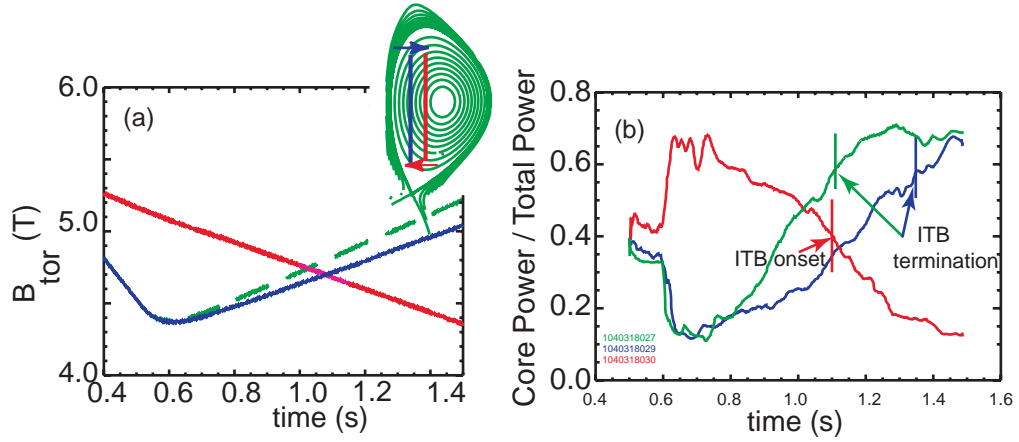


**Fig. 7.**

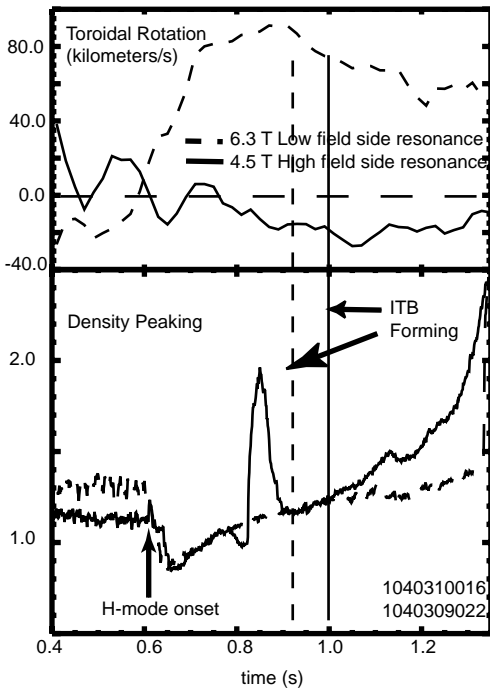


**Fig. 8.**

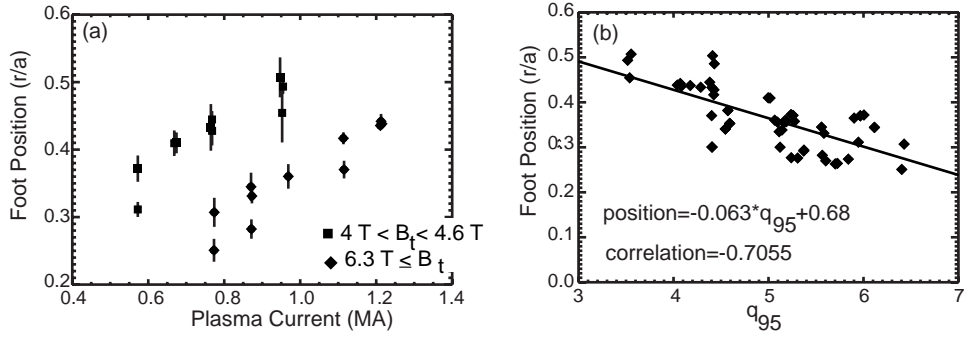


**Fig 9.**